Solution structure of coactosin reveals structural homology to ADF/cofilin family proteins

Maarit Hellman[a], Ville O. Paavilainen[b], Perttu Naumanen[b], Pekka Lappalainen[b], Arto Annila[a], Perttu Permi[a,*]

[a] *Program in Structural Biology and Biophysics, Institute of Biotechnology, University of Helsinki, Finland*
[b] *Program in Cellular Biotechnology, Institute of Biotechnology, University of Helsinki, Finland*

Received 6 July 2004; revised 17 August 2004; accepted 31 August 2004

Available online 11 September 2004

Edited by Amy McGough

Abstract Coactosin is a small (MW ~15 kDa) evolutionarily conserved actin filament binding protein. It displays remote sequence homology to ADF/cofilin proteins and to the ADF-H domains of twinfilin and Abp1/drebrin. However, biochemical analyses have demonstrated that coactosin has a very different role in actin dynamics from the ones of ADF/cofilin, twinfilin or Abp1/drebrin. To elucidate the molecular mechanism of coactosin/actin interaction, we determined the three-dimensional structure of mouse coactosin by multidimensional NMR spectroscopy. We find that the coactosin structure is homologous to ADF/cofilin and to the ADF-H domains of twinfilin. Furthermore, the regions that have been shown to be important for actin filament interactions in ADF/cofilins are structurally conserved in coactosin suggesting that these two proteins interact with F-actin through a conserved interface. Our analysis also identifies key structural differences between these proteins that may account for the differences in biochemical activities and cellular roles of these proteins.

Keywords: Solution structure; ADF; Cofilin; Coactosin

1. Introduction

Dynamic changes in the actin cytoskeleton of eukaryotic cells are regulated by a large number of actin-binding proteins. Many of these proteins have evolved as a result of gene duplications and thus they are composed of a small number of actin-binding motifs. One of the most characterized actin-binding motif is the ADF homology (ADF-H) domain, which is present in at least three distinct groups of actin binding proteins: ADF/cofilins, twinfilins, and Abp1/drebrins [1]. Each group of ADF-H proteins shows unique actin-binding properties and biological activities. ADF/cofilins are small (15–20 kDa) essential proteins that are entirely composed of one ADF-H domain. They bind both filamentous and monomeric actin and promote rapid actin dynamics by severing filaments and catalyzing the dissociation of actin monomers from the filament pointed ends [2]. Twinfilins consist of two ADF-H domains separated by a short linker region. In contrast to ADF/cofilins, twinfilins bind only monomeric actin. The exact biological role of twinfilins is unknown, but they have been proposed to contribute to cytoskeletal dynamics by sequestering actin monomers and by localizing them to the sites of rapid actin assembly in cells [3,4]. Abp1/drebrins are relatively large proteins consisting of an N-terminal ADF-H domain, a variable region, and a C-terminal SH3 domain. These proteins bind only filamentous actin. Biochemical and genetic studies on yeast Abp1 have shown that this protein links Srv2/CAP family of actin monomer binding proteins to actin filaments and promotes actin filament nucleation through the activation of Arp2/3 complex [5–7].

In addition to the three classes of ADF-H domain proteins described above, also a fourth class of proteins, coactosins, may contain an ADF-H domain. However, due to low sequence homology to other ADF-H domain proteins and due to the lack of certain key sequence features, it has been unclear if coactosin is indeed an ADF-H domain protein. Coactosin was originally identified as a 17 kDa protein copurifying with *Dictyostelium discoideum* actomyosin complexes [8]. More recently, coactosin homologs have been identified from *Drosophila*, *Xenopus* and mammals [9]. Similarly to ADF/cofilins, coactosin is composed of only one putative ADF-H domain. The amino acid sequences of coactosins from different species are 15–25% identical to other ADF-H family members, showing the highest level of homology with the N-terminal ADF-H domain of Abp1. Biochemical studies demonstrated that coactosins bind actin filaments with relatively weak affinity and do not interact with actin monomers [8,9]. *Dictyostelium discoideum* coactosin was also reported to show a weak uncapping activity [10]. In addition, Provost et al. [11] demonstrated that mouse coactosin binds 5-lipoxygenase, an enzyme involved in leukotriene biosynthesis, although the biological role of this interaction is unknown. First cell biological studies suggest that coactosin colocalizes with the actin cytoskeleton in cultured cells [8,9]. However, the cell biological role and the mechanism by which coactosin contributes to cytoskeletal dynamics are currently unclear.

* Corresponding author. Fax: +358-9-191-59541.
E-mail address: perttu.permi@helsinki.fi (P. Permi).

Abbreviations: ADF, actin depolymerizing factor; HSQC, heteronuclear single quantum coherence; NOE, nuclear Overhauser enhancement; NOESY, NOE spectroscopy; TROSY, transverse relaxation optimized spectroscopy

0014-5793/$22.00
doi:10.1016/j.febslet.2004.08.068

To assess structural similarity between coactosin and other ADF-H domain proteins, we determined the solution structure of mouse coactosin by NMR spectroscopy. Our results confirm that the overall three-dimensional fold of coactosin is the typical ADF-H domain fold. The actin filament binding regions of ADF/cofilins are also well conserved in the structure of coactosin. However, we also identified structural differences between coactosin and other ADF-H domain proteins and propose that these may account for the differences in the actin-binding characteristics between these actin regulatory proteins.

2. Materials and methods

2.1. Expression and purification of the mouse coactosin

Recombinant mouse coactosin (GenBank Accession No. AI325867) was expressed in *E. coli* BL21(DE3) cells, transformed with a pRAT5 plasmid containing the coactosin gene. Cells were grown in M9 media containing either $^{15}NH_4Cl$ (1 g/l) or $^{15}NH_4Cl$ (1 g/l) and ^{13}C-glucose (2 g/l) as the sole sources of nitrogen and carbon, respectively.

The high-speed supernatant was first loaded onto a Q-Sepharose Fast Flow anion exchange column (Pharmacia) in 20 mM Tris–HCl, pH 8.0, and eluted with a linear NaCl gradient from 0 to 1 M NaCl. The fractions containing the coactosin protein were then applied to a CHT II Hydroxyl-apatite column (Bio-Rad) and eluted with a linear KPO_4 gradient from 0 to 250 mM KPO_4, pH 7.0. After this, the purest fractions were concentrated to less than 2 ml and applied to a Superdex 75 16/60 gel filtration column in 50 mM NaCl, 0.1% NaN_3, 10 mM Bis–Tris, pH 6.0, from where it eluted as a single peak at around 70 ml volume, indicative of a monomeric protein. All samples were subsequently concentrated to 1–1.2 mM solution and verified (mass-spectrometry) to be >99% ^{15}N- or ^{15}N, ^{13}C-labeled. The yield of purified protein was 55 mg/liter, which was comparable to the yield obtained from expression in rich medium.

For the NMR studies, samples of 1–1.2 mM coactosin in 10 mM Bis–Tris (pH 6.0), 50 mM NaCl, 1 mM DTT and H_2O/D_2O (9:1) were prepared. For the amide proton exchange studies protein was lyophilized and dissolved in D_2O. Residual dipolar couplings (RDC) were measured in filamentous phage (Pf1) liquid-crystalline medium at a concentration 4.5 mg/ml with 10 mM Bis–Tris buffer, pH 6.5, and 50 mM NaCl.

2.2. NMR spectroscopy

All spectra were acquired at 25 °C using Varian INOVA 600 and 800 MHz spectrometers. The sequence-specific resonance assignments of $^1H/^{13}C/^{15}N$ nuclei were obtained with completeness over 98% [12]. In addition, methyl proton assignments were confirmed by using 3D DE-MQ-(H)CCMHM-TOCSY spectrum [13]. A complete assignment of aromatic side-chains was facilitated by the identification of aromatic δ protons from (HB)CB(CGCD)HD [14]. The remaining aromatic protons were assigned using 2D ^1H–^1H-nuclear Overhauser enhancement spectroscopy (NOESY), recorded with 80 and 100 ms mixing times from the sample dissolved in 100% D_2O and 3D NOESY-^{13}C-heteronuclear single quantum coherence (HSQC) spectra.

The distance information was collected using 3D NOESY-^{15}N-HSQC [15] and NOESY-^{13}C-HSQC [16], modified to excite aliphatic and aromatic ^{13}C resonances simultaneously, with 100 ms mixing times. $^1D_{HN}$ and $^1D_{C\alpha C'}$ RDCs were obtained using the spin-state-selective transverse relaxation optimized spectroscopy (TROSY) [17] and HNCO(α/β-C′C^α-*J*) [18] experiments. $^1D_{NC'}$ and $^2D_{HNC'}$ dipolar couplings were measured using the HN(α/β-NC′-*J*)-TROSY experiment [19].

The data sets were processed using the Vnmr software package (Varian Inc., Palo Alto, CA, USA) and analyzed by Sparky version 3.106 [20]. The ^{15}N longitudinal (T_1) and transverse (T_2) relaxation data were collected as described earlier [21]. Nine time points per series, delays ranging from 0.01 to 2.1 s for T_1 and from 10 to 250 ms for T_2, were used for non-linear sampling of relaxation. The relaxation times were calculated by fitting cross peak intensities to a single exponentially decaying function using the Sparky software.

2.3. Structure determination and analysis

NOE cross peaks, obtained from two 3D NOESY spectra, were assigned using the NOEASSIGN algorithm of CYANA 2.0.26 [22]. The standard protocol of seven cycles of iterative NOE assignments and structure calculations resulted in a total of 2435 NOE upper distance limits. 135 torsion angle restraints were generated with the program TALOS [23]. From the family of 100 calculated structures, 15 with lowest target function were selected for further refinement and analysis.

In total, 64 $^1D_{HN}$ and 56 $^1D_{CACO}$ RDCs were included in structure refinement using the simulated annealing and energy minimization protocols in the program XPLOR-NIH [24]. Substantial line broadening in the Pf1 liquid crystal medium allowed us to collect only limited set of RDCs with a sufficient precision. All the RDCs were normalized to $^1D_{HN}$. The axial component of alignment tensor $A_\parallel$ and rhombicity R were obtained using the extended histogram method (EHM) [25] to give $A_\parallel = -10.26$ and $R = 0.59$ that were used in the refinement. Additional 27 hydrogen bond restraints were defined on the basis of slowly exchanging amide protons and regular secondary structure elements analyzed from structures calculated with CYANA.

3. Results

3.1. Structure determination of coactosin

In the structure determination based on NOEs, the CYANA program was able to define 2435 distance limits from the total number of 5249 observed NOE cross peaks. The root mean square deviation (RMSD) for the backbone atoms N, CA, CO (residues 3–130) was 0.76 Å and for the backbone heavy atoms 1.14 Å. When the disordered loop region between the β-sheets 4 and 5 (residues 65–73) was excluded, the corresponding RMSD values were 0.39 and 0.84 Å, respectively. Structural statistics is summarized in Table 1. The structure with the lowest CYANA target function value was refined against RDCs. Also hydrogen bond restraints were used in the refinement. Owing to the small number of RDCs the precision did not improve (see Table 1). Consequently, the RDCs served for the structure validation.

3.2. Description of the structure

The resulting structure of coactosin (PDB id, 1wm4) shares the fold typical to ADF domains. There are five internal β-sheets, i.e., β1 (residues 26–32), β2 (residues 35–42), β3 (residues 57–64), β4 (residues 75–82) that are anti-parallel and β5 (residues 110–114) that runs parallel to β4. The β-sheets are surrounded by four α-helices, i.e., α1 (residues 7–16), α2 (residues 45–51) and α3 (residues 88–103) that are parallel to β-sheets, and α4 (residues 122–131), which packs perpendicular to the β3 and β4-sheets. The C-terminal residues 132–142 are disordered (Fig. 1) and flexible on the basis of relaxation data.

The hydrophobic core residues of the protein were identified using the criterion of the solvent accessible surface less than 10% and that amide proton of the residue is in slow exchange with water. Core includes residues Ile5, Cys10, Ala13, Tyr14, Val17, Trp26, Val27, Phe29, Tyr31, Ile36, Tyr45, Phe48, Cys52, Leu58, Phe59, Ala60, Phe61, Val62, Phe64, Phe76, Ala77, Leu78, Ile79, Trp81, Thr94, Phe112, Ile114, Leu120 and Ile125.

3.3. Comparison with other ADF-H domains

The three dimensional structure of coactosin is similar to yeast cofilin (PDB id, 1cfy) [26] with RMSD 2.2 Å, and to the N-terminal domain of mouse twinfilin, N-twinfilin (1m4j) [27] 2.9 Å (Fig. 2B) although the amino acid sequence

Table 1
Structural statistic for the family of 15 structures of coactosin

	NOEASSIGN/ CYANA	XPLOR
NOE upper distance limits		
Total	2435	
Sequential	1281	
$1 < \|i-j\| \leqslant 4$	422	
$\|i-j\| \geqslant 5$	732	
Additional angle restraints used in CYANA[a]		
Distance constraint violation		
Number >0.5 Å	1	0
Torsion angle constraint violation		
Number >5°	0	0
Coordinate precision[a] (Å)		
Res. 3–130		
Backbone	0.74	0.92
All heavy atoms	1.14	1.43
Res. 3–66, 73–130		
Backbone	0.39	0.64
All heavy atoms	0.84	1.19
Ramachandran analysis[b] (%)	Ensemble	
Most favored	77.1	70.7
Additionally allowed	22.6	23.5
Generously allowed	0.3	3.9
Disallowed	0.0	1.9
Target function value (Å^2) (CYANA)		
Averave/best	1.68/1.31	
RMSD from idealized geometry (XPLOR)		
Bond lengths (Å)		0.002 ± 0.0001
Bond angles (°)		0.30 ± 0.01
Improper torsions (°)		0.30 ± 0.02
RMSDs from experimental restraints		
NOE distance constraints (Å)		0.03 ± 0.002
Dihedral constraints (°)		0.57 ± 0.20
Dipolar coupling constraints (Hz)		0.71 ± 0.04

[a] Ramachandran angle constraints for 131 and rotamer angle constraints for 200 residues were obtained, which improves the coordinate precision significantly.
[b] Calculated using PROCHECK-NMR [35].

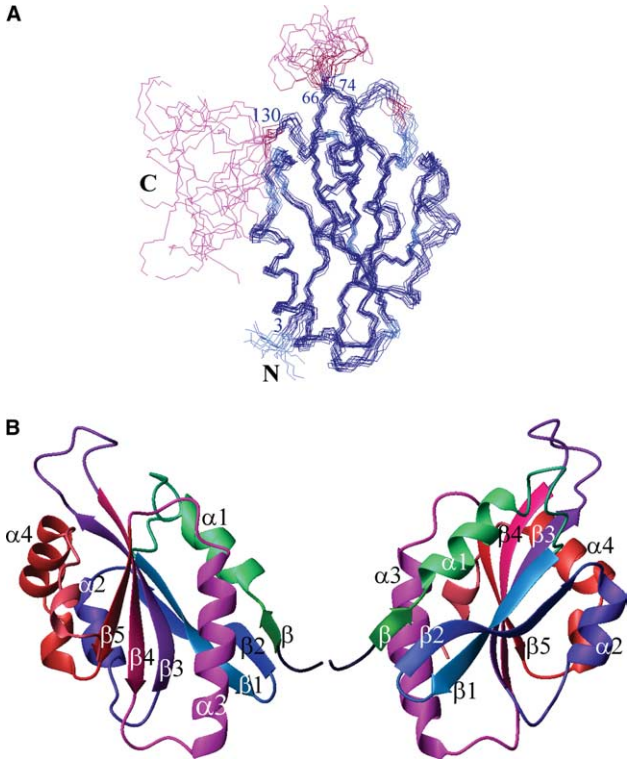

Fig. 1. Overall structure of the coactosin protein. (A) Main chain representation of the (15) lowest energy structures superimposed on one another. Residues are color-coded according to the T_2 relaxation times. Dark blue represents the residues with T_2 close to the mean value (region indicated with residue numbers), violet when 35–90% and magenta when over 90% increase in T_2's were observed and light blue when not measured. (B) A schematic ribbon representation of coactosin. The structure is colored from green (N-terminus) via blue to red to orange (C-terminus). (C) Same as (B) after a 120° rotation relative to the vertical axis. This and all subsequent figures were produced with the program MOLMOL [33] unless otherwise stated.

homology of the coactosin with the other ADF-H domains is less than 25%.

The residues important for F-actin binding are structurally conserved, including Lys72 and Lys75, corresponding to Lys79 and Lys82 in cofilin. The minor differences in the actin binding surfaces of coactosin, cofilin and N-twinfilin, are caused by the substitution of the amino acids important for G-actin binding in the region of long α3-helix.

The conserved tyrosines, present in ADF/cofilins' structures, i.e., Tyr64 and Tyr101 in yeast cofilin, are suggested to stabilize and orient the long α3-helix. Hydrogen bond is suggested between the side chain hydroxyl of Tyr64 and the main chain carbonyl of Tyr101. In coactosin, these residues are substituted by Phe59 and Thr94 with the absence of corresponding hydrogen bond. However, structural fold of the coactosin is maintained by different packing to where Tyr31 (β1-sheet) is also involved. The side chain of Tyr31 lies close to Thr94 in the same location as the aromatic ring of Tyr101 of cofilin, but in a perpendicular orientation (Fig. 3). Hydroxyl of the Tyr31 side chain is pointing towards the face of phenyl group of the Phe59 while hydroxyl of the Thr94 side chain is pointing towards the face of phenol group of the Tyr31. In spite of distinct stabilization mechanisms, distances between the main chains of α3-helix and β3-sheet are equal in coactosin and cofilin. Totally solvent exposed Ile36 (β2-sheet) is also sandwiched between the α3-helix and the core of the protein. The conserved phosphorylation site Ser4 in cofilin is replaced with Thr3 in coactosin, which lies close to the α3-helix. The phosphorylation is not proven for coactosin.

4. Discussion

The solution structure proves that coactosin has the same fold of ADF/cofilins and the N-twinfilin [26,27]. Thus, it belongs to the same ADF-H protein family as ADF/cofilins, twinfilins and Abp1/drebrins and should be considered as the fourth member to this protein family.

Comparison with other known ADF-H domains revealed conservation in the surface residues known to be important for actin filament interactions in ADF/cofilin proteins [28,29]. Furthermore, the structural alignment of coactosin with yeast cofilin verifies that Lys75, which was previously reported to be essential for actin binding in coactosin [9], corresponds to Lys82 of cofilin. Mutagenesis studies have demonstrated that in cofilin this residue is imperative to the actin filament binding [28]. Also, the chemical character of the actin-binding surface of ADF/cofilins and coactosin are similar to each other. This

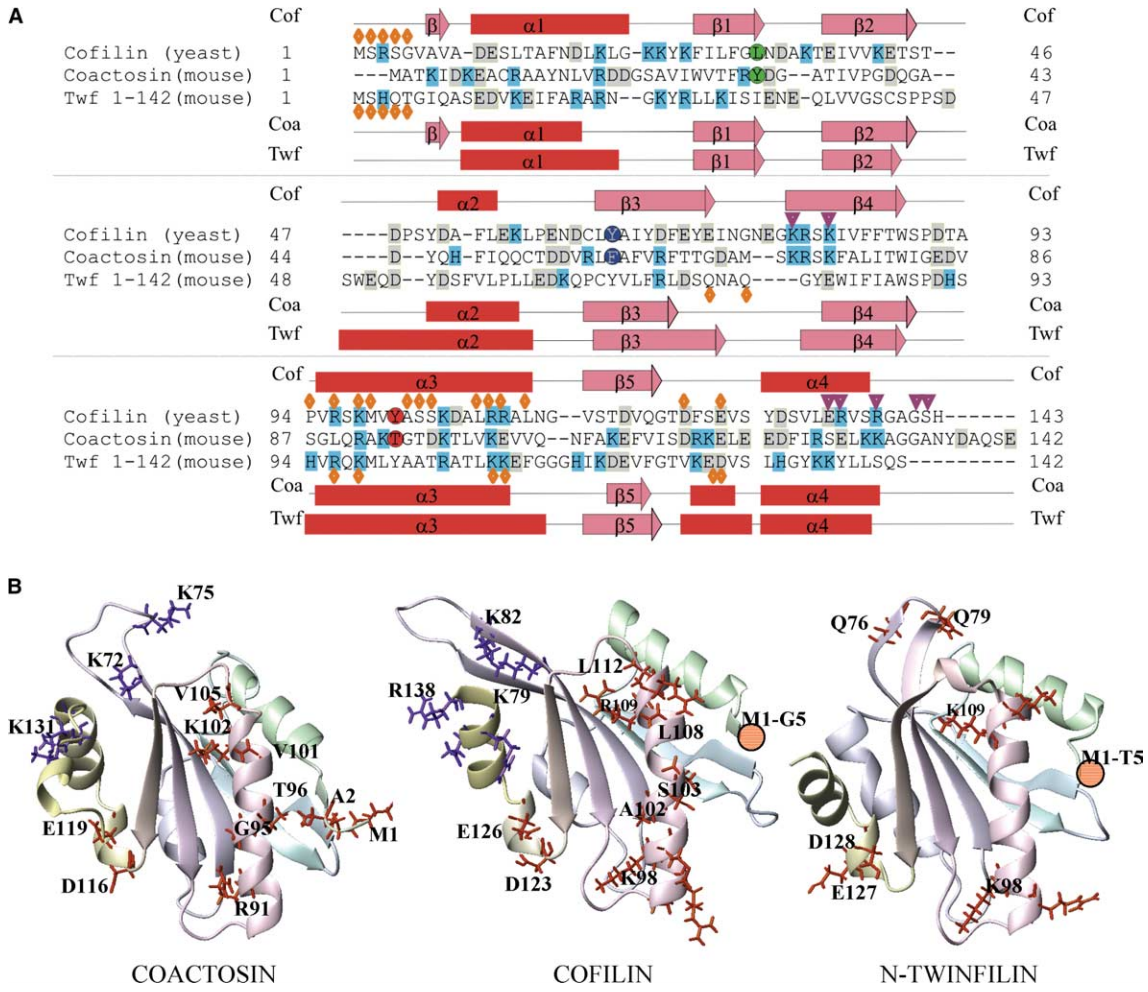

Fig. 2. Structural comparison of coactosin, yeast cofilin and N-twinfilin. (A) Structural sequence alignment. The secondary structure elements of cofilin, coactosin and N-twinfilin are indicated above and below the sequences. Acidic and basic amino acids are color-coded with light blue and grey rectangles, respectively. The residues that have been shown to be important to actin monomer and filament interactions in ADF/cofilins and N-twinfilin are marked with orange diamond and violet triangle, respectively. The key residues for α3-helix stabilization in ADF-H domains and corresponding residues in coactosin (the residues represented in Fig. 3) are marked with circles. (B) Ribbon diagrams of coactosin, cofilin (residues 6–138 shown, crystal structure) and N-twinfilin (residues 7–139 shown, crystal structure). The side chains of the residues important for F-actin and G-actin binding in cofilin are color-coded as in (A). Also the residues conserved in coactosin are indicated with the same color scheme and the corresponding residues are labelled to cofilin and N-twinfilin. Orange colored circles schematically indicate positions of N-terminal residues of cofilin and N-twinfilin involved in G-actin binding. Aligned secondary structure elements of the three proteins are equally colored. Structure-based superposing was applied with the program DALI [34].

suggests that coactosin and cofilin interact with F-actin through the conserved interface.

ADF-H domains have a common mechanism for the stabilization of the long α3-helix, which is based on the highly conserved tyrosines (Tyr64 and Tyr101). The sequence of the coactosin lacks these particular residues, however, the stable fold and the typical orientation of α3-helix isachieved by a distinct packing mechanism.

Interestingly, coactosin binds to actin filaments with significantly lower affinity than ADF/cofilins. Under physiological conditions, the affinity of *Dictyostelium* coactosin to F-actin is ~3 μM [8] and the one of mammalian coactosin is approximately 10 μM [30, Naumanen et al., unpublished]. Under similar conditions the affinities of ADF/cofilins to F-actin are ~0.5–1 μM [31,32]. However, in cells coactosin localizes to certain actin filament structures (Naumanen et al., unpublished) indicating a strong connection between coactosin and actin filaments in cells. This suggests that in vivo the localization of coactosin to actin filaments may be enhanced by interactions with other proteins or by post-translational modification(s) that will increase its affinity to actin. Small structural differences between cofilin and coactosin that were revealed in this study may thus be responsible for coactosin's relatively weak actin affinity in vitro. We propose that activation of coactosin in cells, either through a post-translational modification or by interaction with other currently uncharacterized protein, changes the conformation of coactosin to more 'cofilin-like' and thus increases its affinity to actin and consequently localizes it to the actin cytoskeleton. In the future it will be important to examine the mechanism of coactosin–actin interaction and to reveal how the activity and localization of coactosin are regulated in cells. These studies will also provide the basis for understanding the role of this highly conserved actin-binding protein in cytoskeletal dynamics and various cell processes.

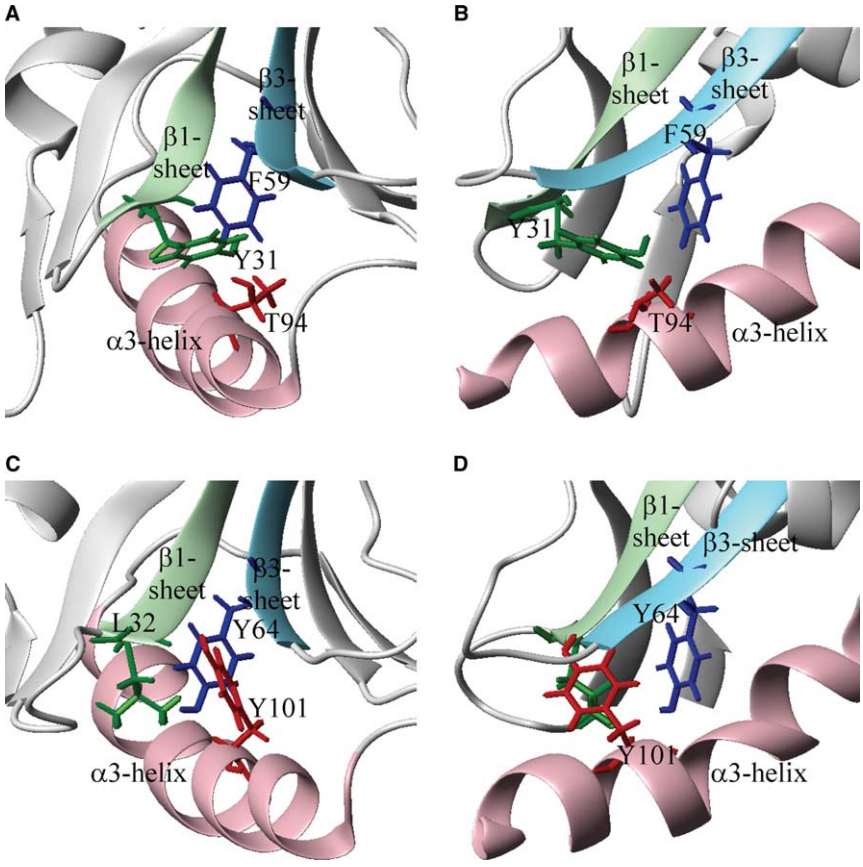

Fig. 3. Representation of the structural basis of the stabilization of the long α3-helix (A) in coactosin and (C) in yeast cofilin (highly conserved in the ADF-H domains). In (B) and (D) are shown the same models as in A and C, respectively, rotated by 90° relative to *y*-axis. Locations of the important residues in the primary structure are shown in Fig. 2A with circles and are colored according to their position. Corresponding secondary structure elements are marked with similar but lighter shading.

Acknowledgements: This study was supported by grants from Academy of Finland (P.L. and P.P.), Sigrid Juselius Foundation, Biocentrum Helsinki, EMBO Young Investigator Program (to P.L.). V.O.P. was supported by a fellowship from Helsinki Graduate School in Biosciences.

References

[1] Lappalainen, P., Kessels, M.M., Cope, M.J.T.V. and Drubin, D.G. (1998) Mol. Biol. Cell 9, 1951–1959.
[2] Bamburg, J.R., McGough, A. and Ono, S. (1999) Trends Cell. Biol. 9, 364–370.
[3] Palmgren, S., Vartiainen, M. and Lappalainen, P. (2002) J. Cell Sci. 115, 881–886.
[4] Falck, S., Paavilainen, V.O., Wear, M.A., Grossman, J.G., Cooper, J.A. and Lappalainen, P. (2004) EMBO J. 23, 3010–3019.
[5] Lila, T. and Drubin, D.G. (1997) Mol. Biol. Cell 8, 367–385.
[6] Goode, B.L., Rodal, A.A., Barnes, G. and Drubin, D.G. (2001) J. Cell. Biol. 153, 627–634.
[7] Balcer, H.I., Goodman, A.L., Rodal, A.A., Smith, E., Kugler, J., Heuser, J.E. and Goode, B.L. (2003) Curr. Biol. 13, 2159–2169.
[8] DeHostos, E.L., Bradtke, B., Lottspeich, F. and Gerisch, G. (1993) Cell Mot. Cytoskel. 26, 181–191.
[9] Provost, P., Doucet, J., Stock, A., Gerisch, G., Samuelsson, B. and Radmark, O. (2001) Biochem. J. 359, 255–263.
[10] Röhrig, U., Gerisch, G., Morozova, L., Schleicher, M. and Wegner, A. (1995) FEBS Lett. 374, 284–286.
[11] Provost, P., Doucet, J., Hammarberg, T., Gerisch, G., Samuelsson, B. and Radmark, O. (2001) J. Biol. Chem. 276, 16520–16527.
[12] Hellman, M., Paavilainen, V.O., Annila, A., Lappalainen, P., and Permi, P. (2004) J. Biomol. NMR (in press).
[13] Permi, P., Tossavainen, H., and Hellman, M., 2004. J. Biomol. NMR (in press).
[14] Yamazaki, T., Forman-Kay, J.D. and Kay, L.E. (1993) J. Am. Chem. Soc. 115, 1054–1055.
[15] Zhang, O., Kay, L.E., Olivier, J.P. and Forman-Kay, J.D. (1994) J. Biomol. NMR 4, 845–858.
[16] Muhandiram, D.R., Farrow, N.A., Guang-yi, X., Smallcombe, S.H. and Kay, L.E. (1993) J. Magn. Reson. B102, 317–321.
[17] Weigelt, J. (1998) J. Am. Chem. Soc. 120, 10778–10779.
[18] Permi, P., Rosevear, P.R. and Annila, A. (2000) J. Biomol. NMR 17, 43–54.
[19] Permi, P. and Annila, A. (2000) J. Biomol. NMR 16, 221–227.
[20] Goddard, T.D. and Kneller, D.G. (2002) Sparky 3. University of California, SF.
[21] Farrow, N.A., Muhandiram, D.R., Singer, A.U., Pascal, S.M., Kay, C.M., Gish, G., Shoelson, S.E., Pawson, T., Forman-Kay, J.D. and Kay, L.E. (1994) Biochemistry 33, 5984–6003.
[22] Güntert, P. (2003) Prog. Nucl. Magn. Reson. Spectrosc. 43, 105–125.
[23] Cornilescu, G., Delaglio, F. and Bax, A. (1999) J. Biomol. NMR 13, 289–302.
[24] Schwieters, C.D., Kuszewski, J.J., Tjandra, N. and Clore, G.M. (2003) J. Magn. Reson. 160, 65–73.
[25] Bryce, D. and Bax, A. (2004) J. Biomol. NMR 28, 273–287.
[26] Fedorov, A.A., Lappalainen, P., Fedorov, E.V., Drubrin, D.G. and Almo, S.C. (1997) Nat. Struct. Biol. 4, 366–369.
[27] Paavilainen, V.O., Merckel, M.C., Falck, S., Ojala, P.J., Pohl, E., Wilmanns, M. and Lappalainen, P. (2002) J. Biol. Chem. 277, 43089–43095.
[28] Lappalainen, P., Fedorov, E.V., Fedorov, A.A., Almo, S.C. and Drubin, D.G. (1997) EMBO J. 16, 5520–5530.

[29] Ojala, P.J., Paavilainen, V.O. and Lappalainen, P. (2001) Biochemistry 40, 15562–15569.
[30] Doucet, J., Provost, P., Samuelsson, P. and Radmark, O. (2002) Biochem. Biophys. Res. Commun. 290 (2), 783–789.
[31] Blanchoin, L. and Pollard, T.D. (1999) J. Biol. Chem. 274 (22), 15538–15546.
[32] Yeoh, S., Pope, B., Mannherz, H.G. and Weeds, A. (2002) J. Mol. Biol. 315, 911–925.
[33] Koradi, R., Billeter, M. and Wuthrich, K. (1996) J. Mol. Graph. 14, 51–55.
[34] Holm, L. and Sander, C. (1995) Trends Biochem. Sci. 20, 478–480.
[35] Laskowski, R.A., Rullmann, J.A.C., MacArthur, M.W., Kaptein, R. and Thornton, J.M. (1996) J. Biomol. NMR 8, 477–486.